



EXPERIMENTAL INVESTIGATION OF REINFORCED CONCRETE WIDE BEAMS – COLUMN JOINTS UNDER CYCLIC LOAD

Alaa F. Elkashif¹, Hamed M. Salem², Hatem H. Ghith³,
Ahmed M. Farahat⁴

1-Research Associate, Reinforced Concrete Research Institute, Housing and Building National Research Center, Giza, Egypt

alaa.elkashif@yahoo.com

2- Professor of Concrete Structures, Structural Engineering Dept., Cairo University, Giza, Egypt
hamedhadhoud@yahoo.com

3- Professor, Reinforced Concrete Research Institute, Housing and Building National Research Center, Giza, Egypt
hatem_ghith@hotmail.com

4- Professor of Concrete Structures, Structural Engineering Dept., Cairo University, Giza, Egypt
dr_farahat@yahoo.com

ملخص البحث :

يشتمل هذا البحث على دراسة سلوك وصلات الكمرات العريضة والاعمدة الخرسانية المسلحة والمعرضة لأحمال دوريه عمليا ولدراسة هذا السلوك تم تصميم برنامج عملي مكون من ستة نماذج لدراسة تأثير المتغيرات و هي عرض الكمرة، توزيع الحديد الرئيسي بالكمرة، وتوزيع الكانات بالكمرات العريضة على حمل الانهيار، ممطولية القطاع، شكل الشرخ، فقد الجساءة و الطاقة. و اظهرت النتائج أن وصلات الكمرات العريضة والاعمدة الخرسانية المسلحة التي صممت طبقا لاشتراطات الزلازل بالكود المصري توفر أداء زلزالي جيد حتى عندما كانت نسبة عرض الكمرة لعرض العمود أكبر من اثنين و ايضا عندما كان ثلثي الحديد الرئيسي خارج قطاع العمود. ولذلك يوصى بتغيير الحدود المسموح بها لعرض الكمرة في الكود المصري مع الأخذ في الاعتبار تأثير الكانات و توزيع الحديد في ممطولية القطاع.

1. Abstract:

This study was carried out to evaluate experimentally the hysteric behavior of reinforced concrete wide beam –column joints when subjected to lateral cyclic loading. In the current study, six wide beam column – joints were tested to investigate the effect of beam width, reinforcement configuration, and stirrups configuration on the ultimate capacity, ductility, cracking pattern, stiffness degradation, and energy dissipation. Based on this study, wide beam – column joints designed according to seismic provision of the Egyptian code provide ductile seismic performance even when beam width to column width is greater than two and when two – thirds of the wide beam flexure reinforcement is anchored outside the column core. Therefore, beam width limit in the Egyptian code may be increased. Stirrups significantly affect the behavior of wide beams.

Keywords: wide beam-column joints, bond, cyclic response, earth quake resistant structure, seismic design, seismic behavior.

2. Introduction

The use of wide beams is popular in hollow block reinforced concrete slabs for its constructional and architectural advantages especially in Egypt. This system provides flexibility and a sense of spacious. It reduces the amount of form work required.

Most design codes [1, 2] placed restrictions on the use of wide beams framing systems in seismic regions because of insufficient information about their behavior under the effects of earthquake loadings and due to lack of data on the anchorage of such bars under large load reversals.

The maximum effective wide beam width according to ECP [1] is the smaller of $b_c + h_b$ and $2b_c$, where b_c is the column width and h_b is the beam depth. On the other hand the max effective beam width allowed by ACI [2] is the smaller of $b_c + 1.5h_c$ and $3b_c$, where h_c is the column length.

Elsouri and Harajli [3] found that when subjecting as-built joints that were detailed without taking earthquake loads into account to cyclic load, wide beam -column joints develop sizable diagonal shear cracks and, then, joint shear failure at a small drift ratios. The specimens didn't reach the estimated lateral load capacities. Elsouri et al. [4, 5, and 6] studied the seismic performance of the joints by improving the reinforcement details. All specimens performed well in spite of beam to column width ratio was higher than three and when more than two thirds of the wide beam main reinforcement was outside the column core. Considerably lower damage within the joint core and the concrete damage in the joints was particularly concentrated within the plastic hinge region of the beams instead of the difficult-to-access joint core makes the repair and strengthening of such joints, after being subjected to strong earthquake load, more feasible. While other studies, Abdel -Rahman, et al [7, 8], found that the effective beam width is less than the beam width when the beam to column width ratio is higher than three.

Experimental results of Fateh, et al. [9] showed that the failure capacity of joints with concentrated longitudinal bars of beam that two-third of bars anchored in the column zone was 24 % higher than even bar distribution. Abdel -Rahman [7] found that concentration of reinforcement in the middle strip (width equal to half the beam width) for beam width to column side of four improve the performance as it increase failure load, cracking load and increase beam stiffness. Hala Metawei [10] reported that the failure load increased due to concentration of beam reinforcement at column strip

Said and Elrakib [11] found that the contribution of web reinforcement to the shear capacity is significant and directly proportional to the amount and spacing of the shear reinforcement, as it improves the contribution of the dowel action, and limiting the opening of inclined shear cracks. There is an increase in the shear capacity of the tested beams compared with the control beam. The shear reinforcement amount enhances the ductility of the wide beams. Also, as the spacing between web reinforcement decreased, the ductility of the specimens was increased. High grade steel was more effective in the contribution of the shear strength of wide beams. They recommended that the contribution of shear reinforcement need to be included in the Egyptian Code requirements for shear capacity of wide beam. As the formula for estimating the shear capacity is highly conservative and should be revised to account for the existence of the web reinforcement.

3. RESEARCH SIGNIFICANCE

The main objective of this research is to investigate and provide analysis of the effect of the major test variables beam width, beam reinforcement concentration at column core, and number of stirrups branch on the behavior of reinforced concrete wide beam – column joints when subjected to lateral earthquake loading.

4. EXPERIMENTAL PROGRAM

Test was carried out on six full scale specimens divided into three groups. In all specimens the column length dimension is parallel to the direction of applying lateral load.

4.1 Test Specimens

Specimens were cast with a beam length of 1150 mm and column height of 2000 mm. Column and beam concrete dimensions and reinforcement are shown in Table 1.

Table 1: Column and beam reinforcement

Specimens	Beam dimensions		Beam reinforcement (ratio) top = bottom	Column dimensions		Column reinforcement (ratio)
	d_b	b_b		b_c	h_c	
J1	200	400	6 Φ 12 (0.997)	200	500	10 Φ 12 (1.13%)
J2, J3, J4		600	6 Φ 12 (0.665)			
J5, J9		800	6 Φ 10 + 2 Φ 12 (0.513)			

The specimen concrete dimensions and reinforcement details are shown in Figure 1 through Figure 6, all dimensions in (mm).

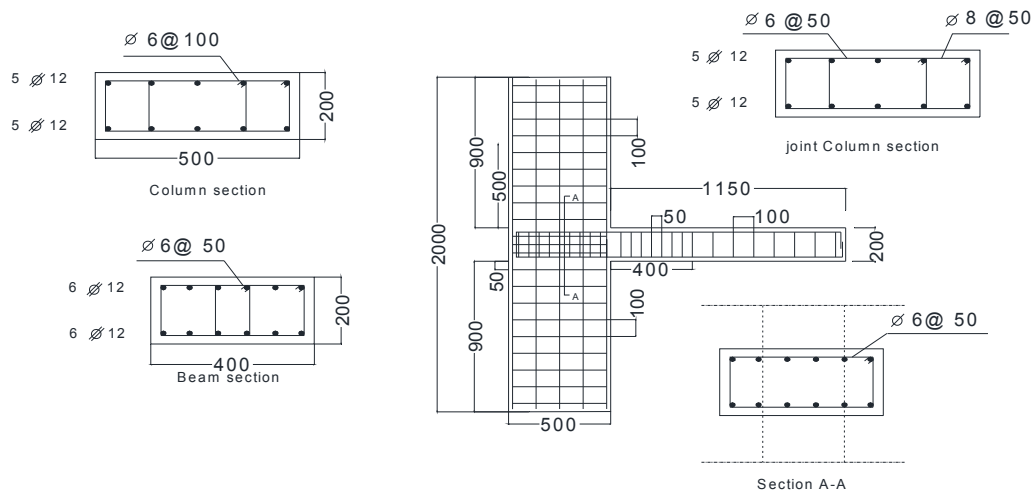


Figure 1: Reinforcement details for specimen J1

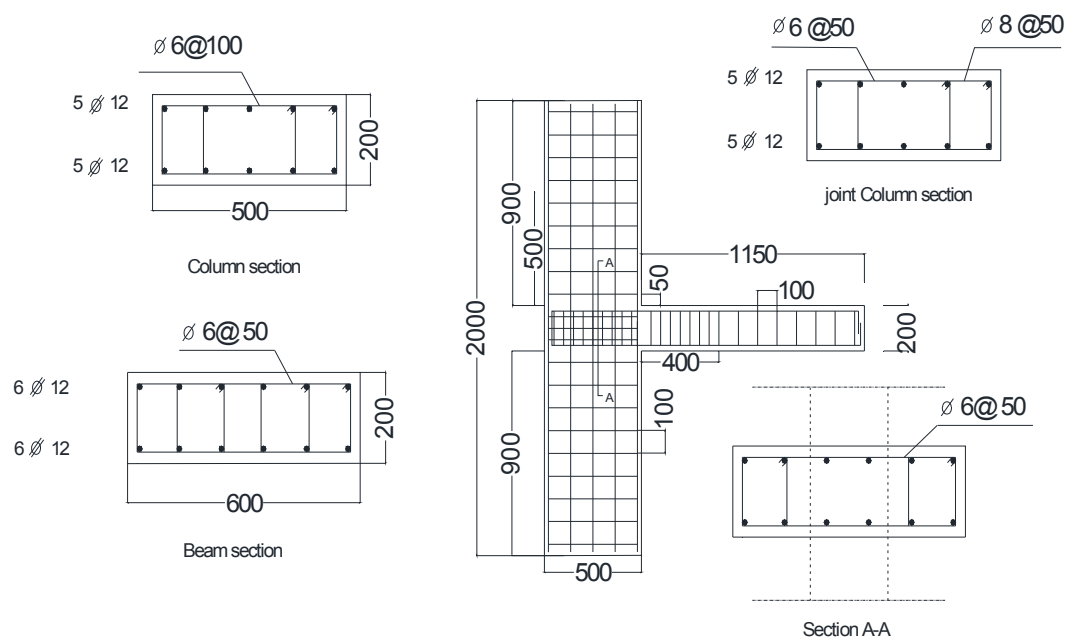


Figure 2: Reinforcement details for specimen J2

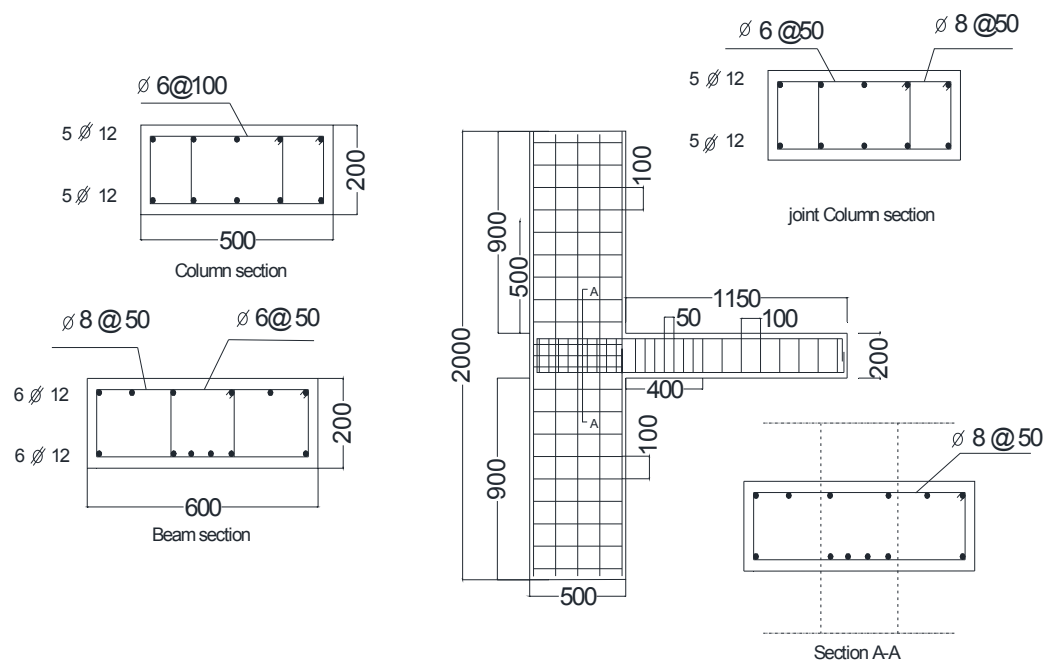


Figure 3: Reinforcement details for specimen J3

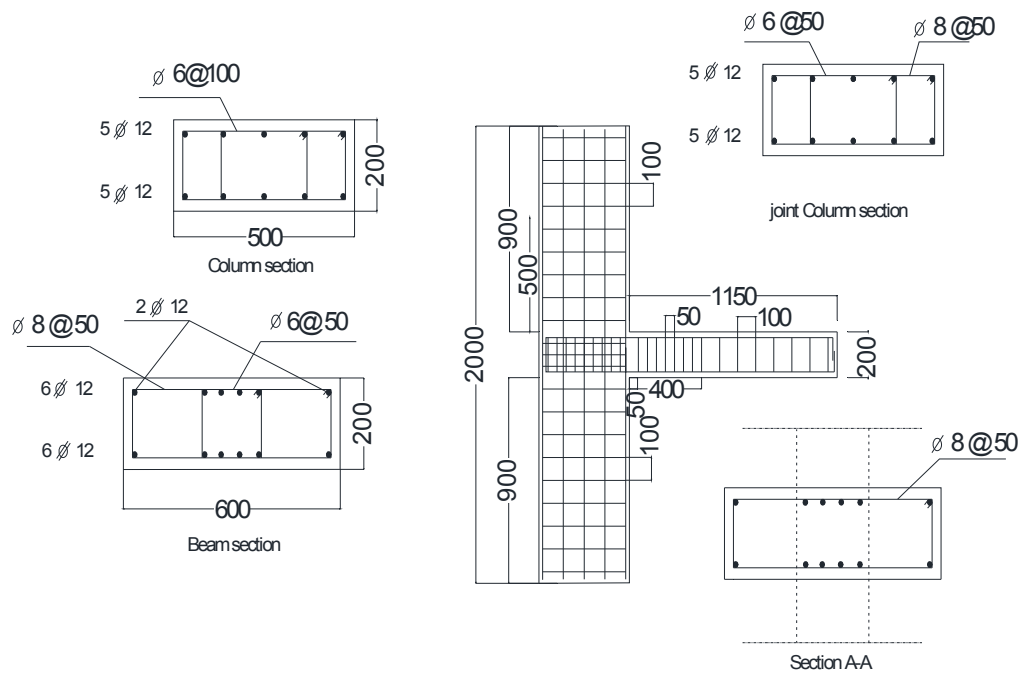


Figure4: Reinforcement details for specimen J4

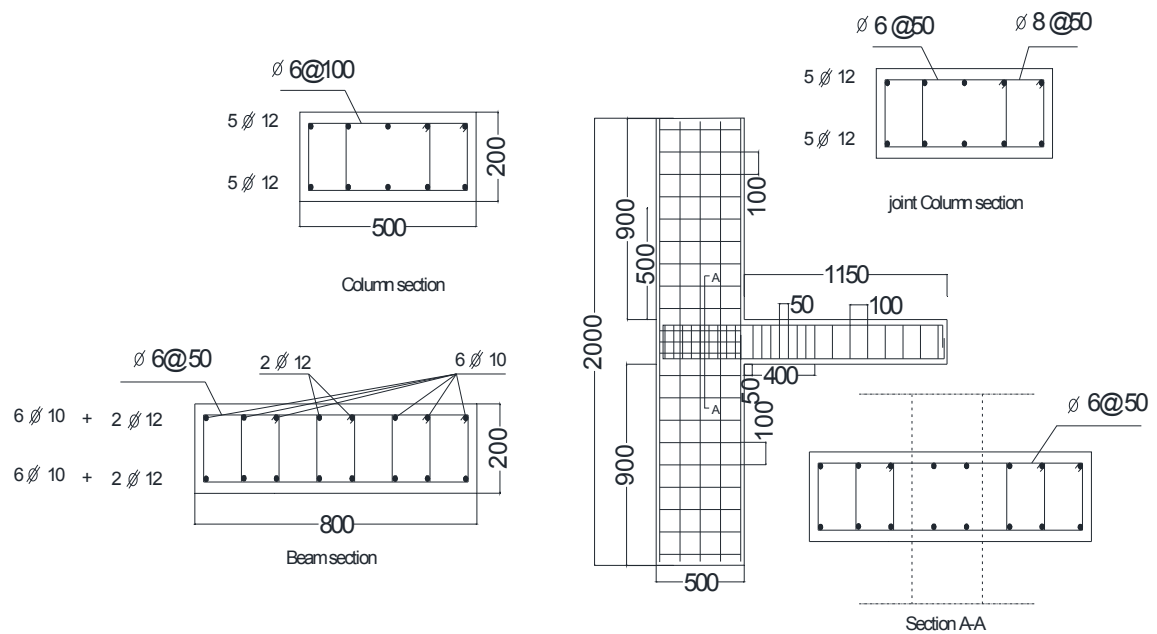


Figure 5: Reinforcement details for specimen J5

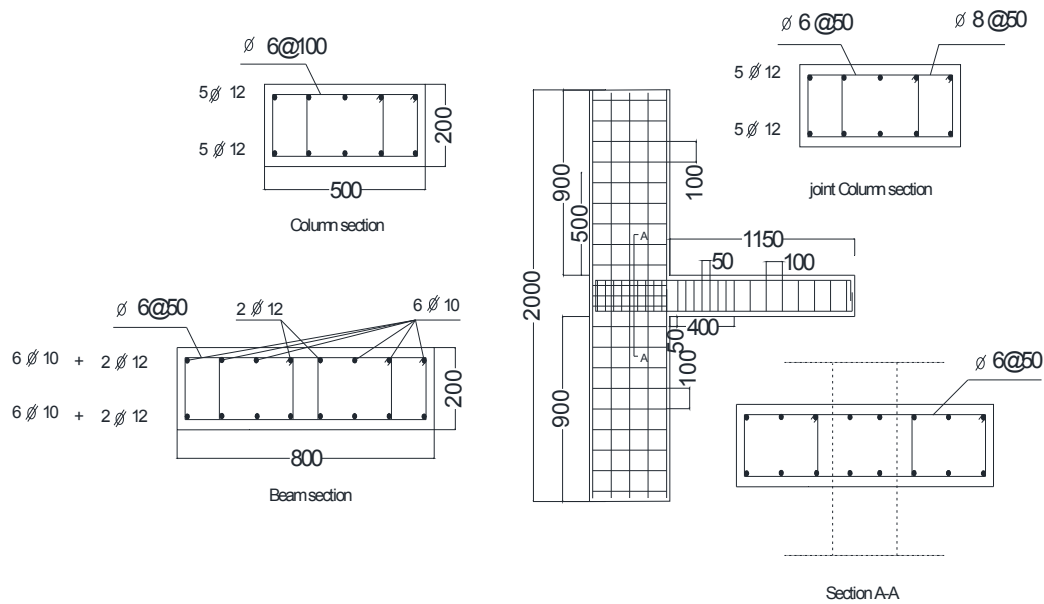


Figure 6: Reinforcement details for specimen J9

4.2 Material Properties

Test specimens were prepared from available local materials. These including cement CEMI (42.5 N), natural sand, crashed dolomite with maximum normal size of 10 mm, and steel reinforcement. Clean drinkable fresh water was used in all mixes and also for curing process. The mix proportions were designed to achieve target strength of 35 N/mm². Table 2 shows design of the concrete mix. Deformed bars with diameters 10, and 12 mm were used as the main reinforcement diameters for both beam and column. Mild steel bars with 6, and 8 mm diameter were used for the column and beam stirrups. Table 3 shows the properties of the steel bars used in this study.

Table 2: Design of The Concrete Mix (per m³)

Cement (kg/m ³)	Coarse aggregate (dolomite) (kg/m ³)	Fine aggregate (Sand) (kg/m ³)	Water (liter)
410	1024	683	240

Table 3: Properties of Steel bars

Properties	Ø 6	Ø 8	Φ 10	Φ 12
Grade	24/35	24/35	40/60	40/60
Shape	Plain bars	Plain bars	Deformed bars	Deformed bars
Yield stress (N/mm ²)	354	338	599	526
Ultimate stress (N/mm ²)	495	468	688	650
Weight per meter length	0.22	0.39	0.62	0.88
Ultimate stress/ Yield stress	1.4	1.38	1.15	1.24
Ultimate strain	0.25	0.23	0.16	0.15

4.3 Test Setup and Instrumentation:

Typical quasi – static test setup is selected for wide beam-column joints testing. Column was supported laterally at two points, to prevent - out – of - plane rotation of column. Axial load approximately $0.15 f_c' A_g$ was applied on column top during the application of cyclic load on beam. First, the column axial load was applied, then the cyclic displacement was applied at the beam tip. Figure 7 shows test setup and instrumentation used for test specimens. The point of loading for all specimens was 1020 mm away from column face. All specimens were subjected to the same loading protocol shown in Figure 8. All cycles of the test were carried out in the displacement control mode. The load is composed of two cycles at each displacement, which varied between 1 mm and 80 mm. All data from the instrument were continuously collected by data acquisition system. The test was continued until the specimen reached 75% of the ultimate load of the specimen.

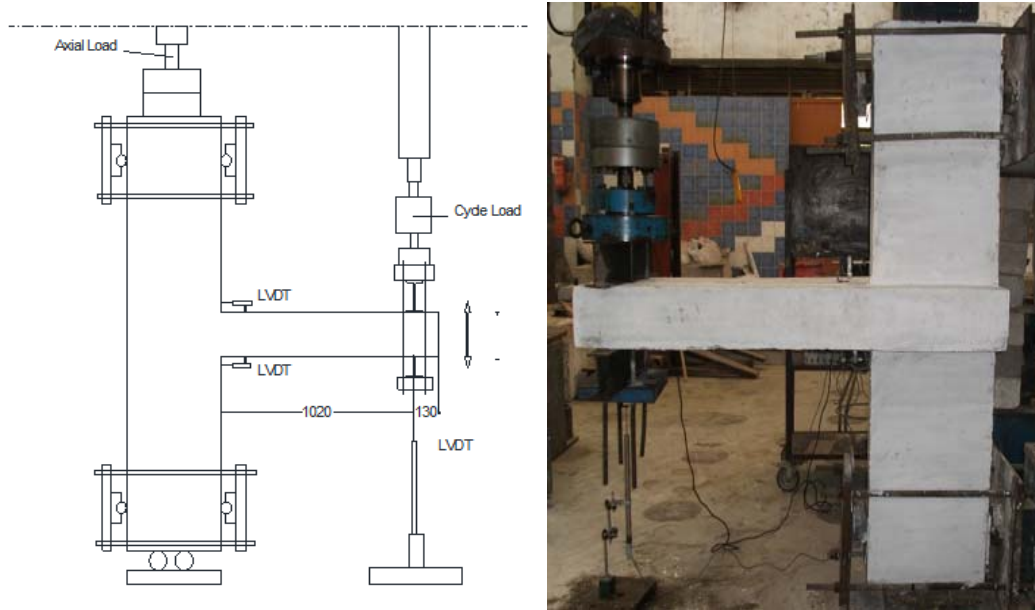


Figure 7: Test setup and Instrumentation used for test specimens

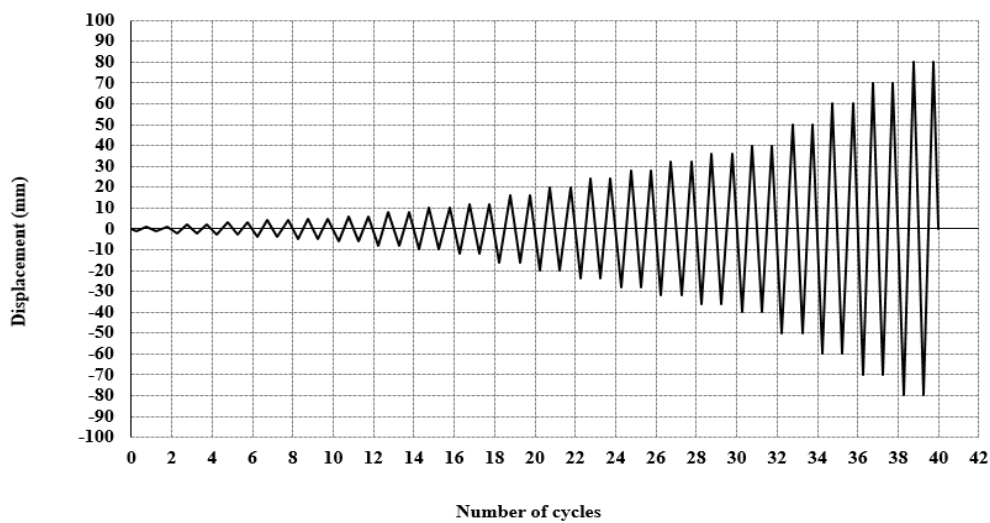


Figure 8: Loading Pattern 1

5. EXPERIMENTAL RESULTS AND DISCUSSION

The concrete cover thickness was different as shown in table 4 due to casting operations which effect the moment capacity of the specimens.

Table 4: Top and Bottom concrete cover in (mm)

Concrete cover	Top	Bottom
J1	15	35
J2	22	25
J3	25	25
J4	25	30
J5	23	29
J9	18	30

5.1 General behavior and mode of failure

Figure 9 through figure 14 show the crack pattern for specimens J1, J2, J3, J4, J5, and J9. The observed cracks weren't symmetric for the top and bottom of the beam and this is due to the different in concrete cover as shown in table 4. The first flexural crack has developed on the top face and on the side of the beam at the joint interface section and continued to develop on the beam sides and spread beyond the face of the column for a distance of approximately 600 to 720 mm. Diagonal shear cracks appears at beam column interface. These diagonal cracks did not indicate any sign of joint shear failure, as their size remained small until the end of the test. The width of the cracks at the face of the column increased causing considerable concrete damage. Splitting cracks developed as well along the outermost bottom bar on the other side of the beam. These splitting cracks widened leading to concrete spalling at the bottom corners of the beam. This was regarded however as a secondary mode of failure as the development of these cracks did not affect the overall response of the specimens.



Figure 9: Crack pattern of specimen J1

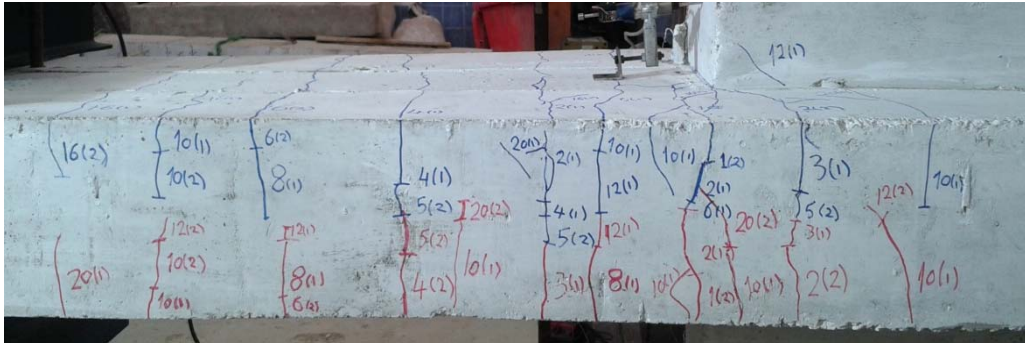


Figure 10: Crack pattern of specimen J2

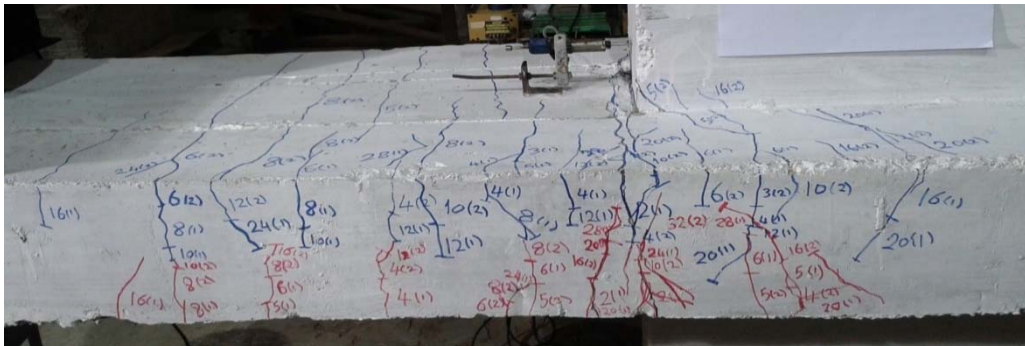


Figure 11: Crack pattern of specimen J3

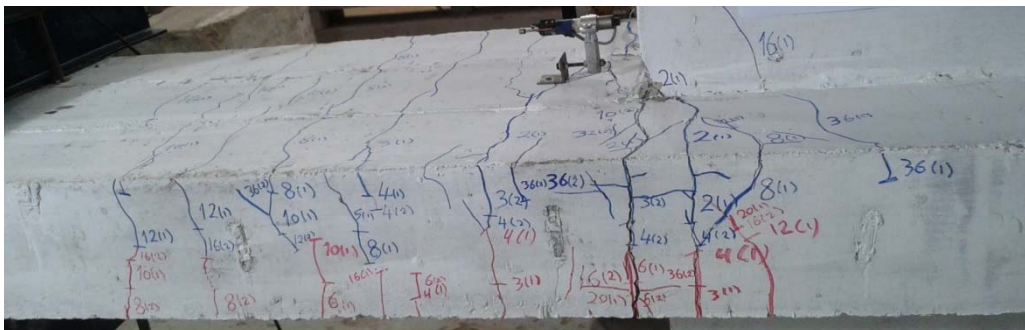


Figure 12: Crack pattern of specimen J4

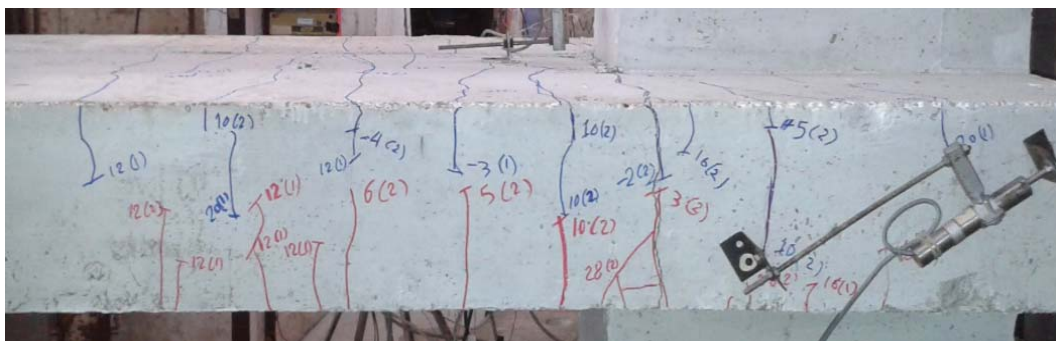


Figure 13: Crack pattern of specimen J5

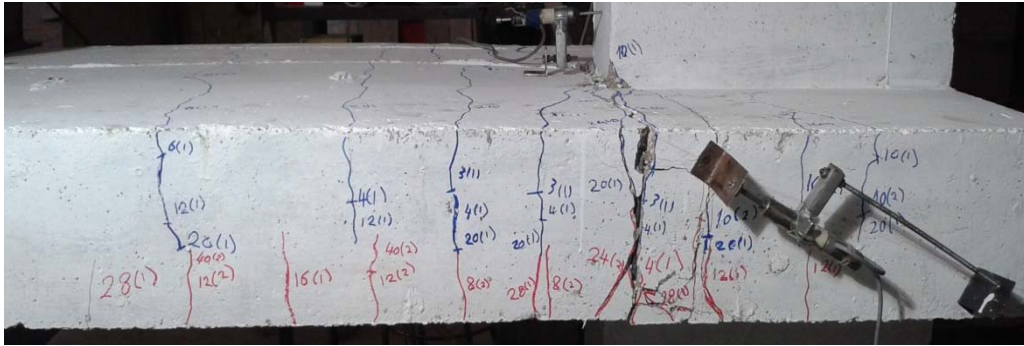


Figure 14: Crack pattern of specimen J9

5.2 Lateral load – drift response

The load – displacement hysteresis loops for the six specimens displayed similar behavior. The unsymmetrical positive and negative cycles of the load displacement response recorded in all specimens is due to the own weight of the beam and due to the test setup. Figures 15 through 17 show Load – versus - displacement hysteric loops for the six specimens.

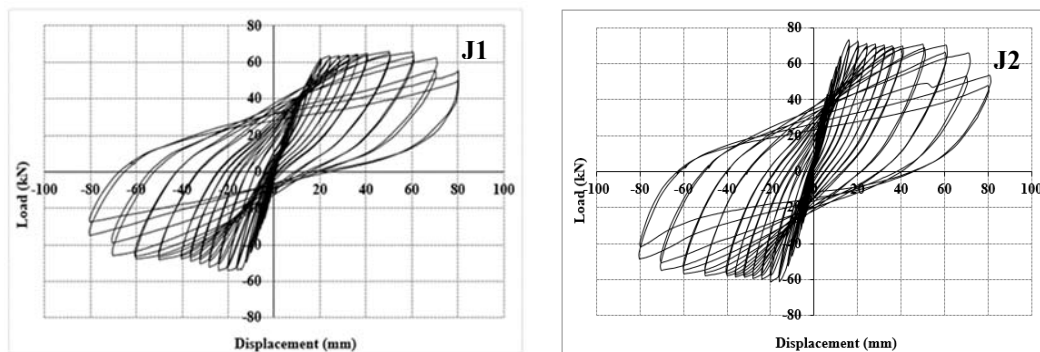


Figure 15: Load displacement hysteric curves for specimen J1, J2

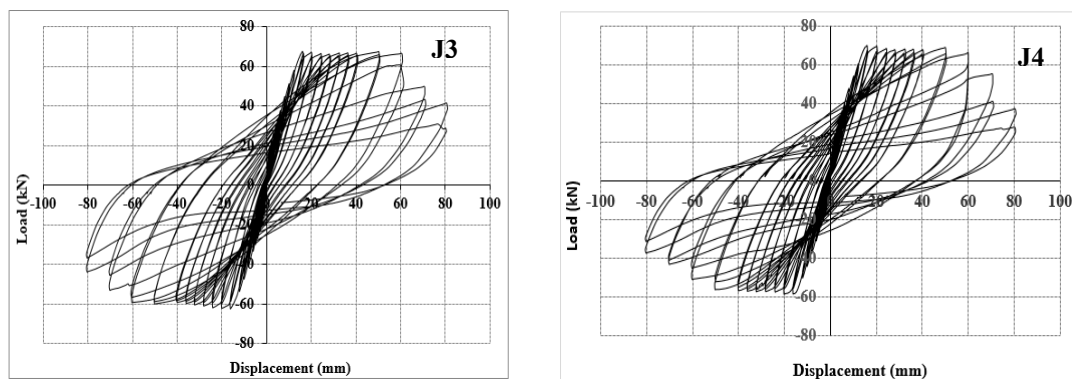


Figure 16: Load displacement hysteric curves for specimen J3, J4

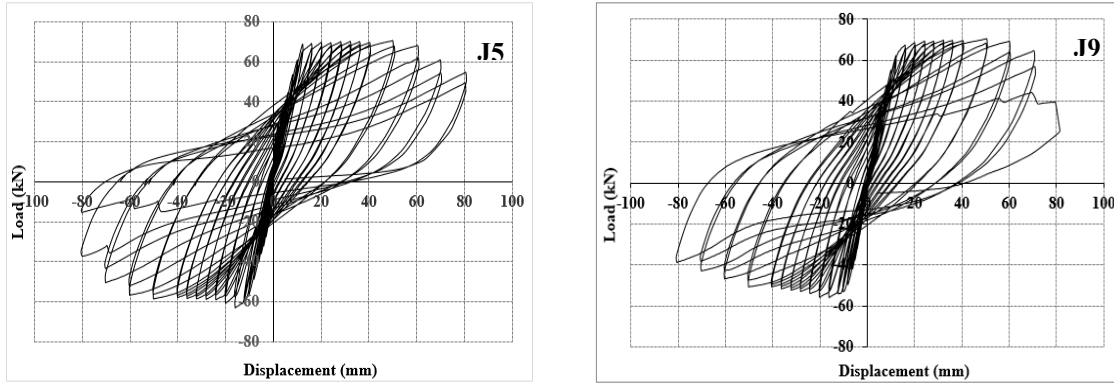


Figure 17: Load displacement hysteric curves for specimen J5, J9

6. Analysis of test variables

This section presents method to evaluate ductility, stiffness degradation rate, and energy dissipation to evaluate the performance of beam- column joints under seismic action

Ductility:

$$\mu = \Delta_{0.85max} / \Delta_y$$

Where Δ_y is the displacement of the equivalent elasto-plastic system with reduced stiffness found as the secant stiffness at 75% of the ultimate lateral load of the real system. Δ_{max} is the post – peak displacement when the load carrying capacity has undergone a small reduction $0.85H_{max}$ where H_{max} is the maximum capacity of the section.

Stiffness degradation rate: the cycle stiffness of the specimens at specified displacement level was considered as the average of the stiffness in the positive and negative loading directions.

$$KDR = \left(\frac{K_o - K_u}{K_o} \right) \%$$

Where K_o and K_u are the flexural stiffness of the specimens at initial and at ultimate levels respectively. All specimens suffered a reduction in stiffness during subsequent displacement cycles. This loss of stiffness is due to concrete deterioration in and adjacent to the joint core.

Energy dissipation: under severe earthquake, beam column joints will suffer from large inelastic deformations. The ability of dissipating the inelastic deformation energy is one of the significant factors for evaluating the performance of beam column joints subjected to seismic action.

The specimens were divided into three groups. Group 1 includes specimens J1, J2 and J5 to study the effect of beam width; group 2 includes specimens J2, J3 and J4 to study the effect of reinforcement concentration; however group 3 includes specimens J5 and J9 to study the effect of stirrups configuration.

6.1 Effect of beam width

To study the effect of beam width on the behavior of reinforced concrete wide beam – column joints, three specimens J1, J2, and J5 with the same steel area but different in beam dimensions (400, 600, and 800 mm) were tested.

Figure 18 shows Load –displacement ductility envelope for group 1. Specimen J1 shows lower ultimate capacity. Relative to expected capacity, the increase in average load capacity was 13.46%, 22.27% and 8.45% for specimens J1, J2 and J5. Relative to J1, increasing width increases lateral load capacity with 12.42% and 11.03% for specimens J2 and J5 as shown in figure 19. Relative to J1, increasing width increases ductility with 12.90% and 31.66% for Specimens J2 and J5, respectively as shown in figure 20.

Figure 21 shows the Cumulative dissipated energy versus displacement at different displacement levels for Group1. Where J1 possesses lower energy dissipation capacity than J2 and J5 and J5 has the best ability to dissipate energy. Comparing the initial stiffness values Clear that J5 which is wider has initial stiffness higher than J1 and J2.

Figure 22 shows the stiffness calculated at different displacement levels for each specimen. The figure shows steady degradation. This degradation is due to the propagation and widening of the flexure cracks.

Relative to J1, the increase in stiffness degradation rate was 5.94% and 6.92% for specimen J2 and J5 as shown in Figure 23, this implies that stiffness degradation rate for specimen J5 is higher than J1 and J2 and this results in reduction in the rate of crack propagation for J5.

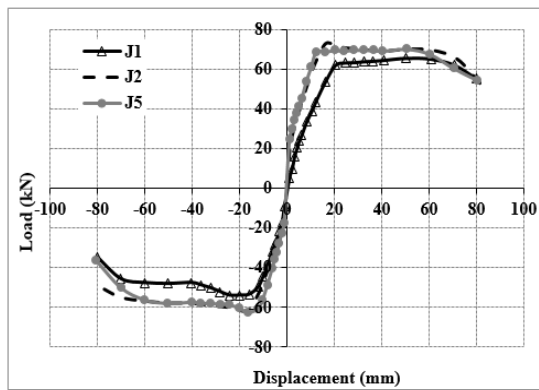


Figure 18: Load –displacement ductility envelope for group 1

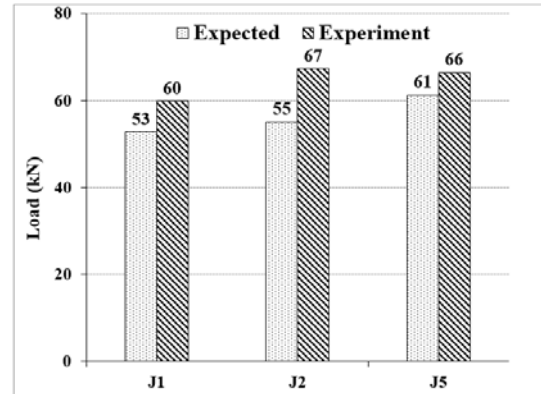


Figure 19: Expected and Experimental load capacities for group 1

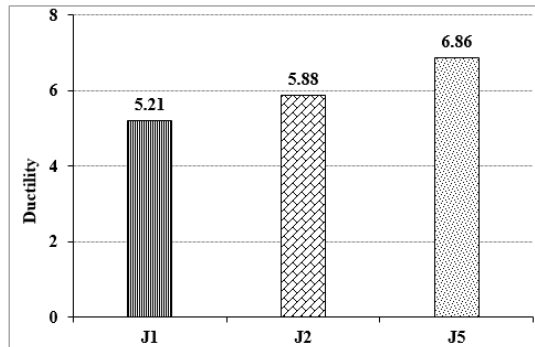


Figure 20: Displacement ductility factor for group 1

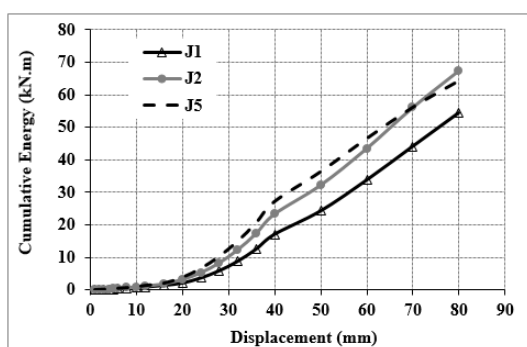


Figure 21: Cumulative dissipated energy versus displacement for group 1

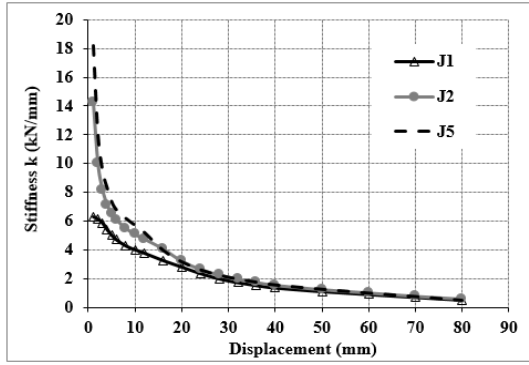


Figure 22: Stiffness degradation versus displacement for group 1

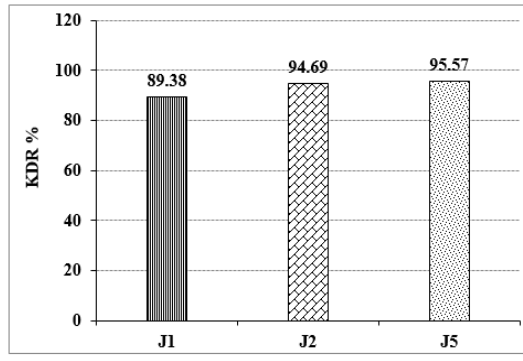


Figure 23: Stiffness degradation rate for group 1

6.2 Effect of reinforcement concentration

To study the effect of beam reinforcement distribution at column core on the behavior of reinforced concrete wide beam –column joints, three specimens (J2, J3 and J4) with the same steel area but different in reinforcement distribution inside column core. J2 uniformly distributed, J3 (with uniformly distributed for top and 0.67 concentration for bottom reinforcement), and J4 (with 0.67 concentration for top and bottom reinforcement) were tested.

Figure 24 shows Load –displacement ductility envelope for group 2. Specimen J4 shows lower ultimate capacity. Relative to expected capacity, the increase in load capacity was 22.27 %, 18.34 % and 18.84 % for specimens J2, J3 and J4. Relative to J2, increasing reinforcement concentration decreased lateral load capacity with 4.09% and 5.04% for specimen J3 and J4 as shown in figure 25. Relative to J2, increasing reinforcement concentration decreases ductility with 12.21% and 14.44 % for Specimens J3 and J4, respectively as shown in figure 26.

Figure 27 shows the Cumulative dissipated energy versus displacement at different displacement levels for group 2. Where J2 possess higher energy dissipation capacity than the J3 and J4 and J2 has the best ability to dissipate energy. Comparing the initial stiffness values clear that J2 which is uniformly distributed had initial stiffness higher than J3 and J4.

Figure 28 shows the stiffness calculated at different displacement levels for each specimen. The Figure shows steady degradation. This degradation is due to the propagation and widening of the flexure cracks.

Relative to J2, the decrease in stiffness degradation rate was 0.93% and 0.56 % for specimens J3 and J4 as shown in Figure 29, this means that stiffness degradation rate for specimen J2 is higher than J3 and J4 and this mean that J2 has a reduced propagation rate of crack.

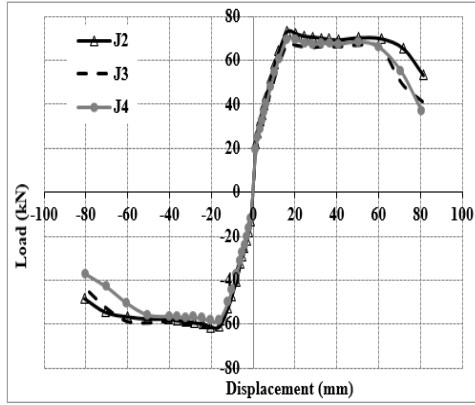


Figure 24: Load –displacement ductility envelope for group 2

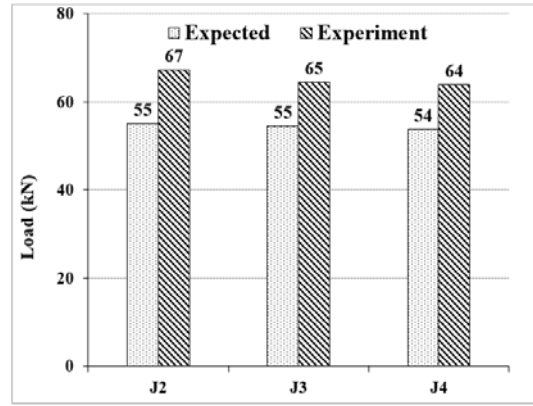


Figure 25: Expected and Experimental load capacities for group 2

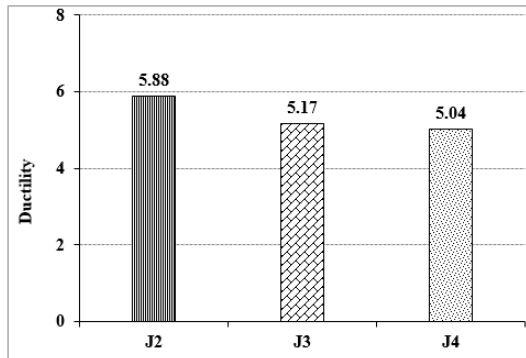


Figure 26: Displacement ductility factor for group 2

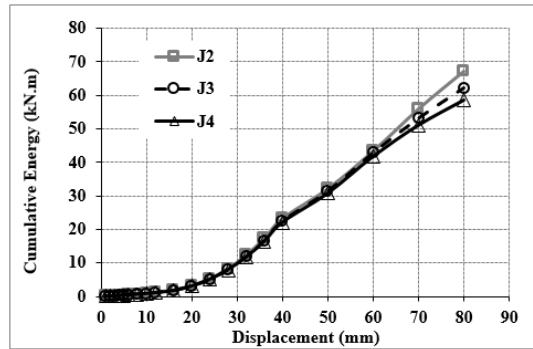


Figure 27: Cumulative dissipated energy versus displacement for group 2

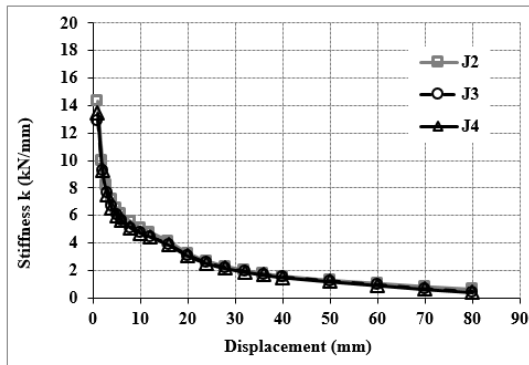


Figure 28: Stiffness degradation versus displacement for group 2

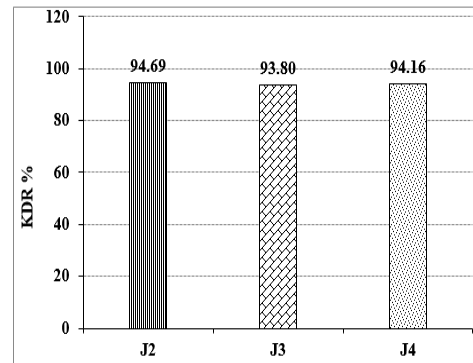


Figure 29: Stiffness degradation rate for group 2

6.3 Effect of Stirrups configuration (number of stirrups branch)

To study the effect of Stirrups configuration (number of stirrups branch) on the behavior of reinforced concrete wide beam –column joints, two specimens (J5, and J9) with the same steel area but different in number of stirrups branch in beam were tested.

Figure 30 shows Load –displacement ductility envelope for group 3. Specimen J9 shows lower ultimate capacity. Relative to expected capacity, the increase in load capacity was 8.45 % and 1.27% for specimen J5 and specimen J9. There is a different in expected lateral load capacity due to different in concrete cover. Relative to J5,

decreasing number of stirrups branch decreases lateral load capacity with 5.2 % for specimen J9 as shown in Figure 31. Specimen J9 showed lower ductility index by 7.48 % compared with that for specimen J5 as shown in Figure 32.

Figure 33 shows the Cumulative dissipated energy versus displacement at different displacement levels for group3 while J5 and J9 have the same energy dissipation capacity. Comparing the initial stiffness values for J5 and J9 shows that J5 had initial stiffness higher than J9.

Figure 34 shows the stiffness calculated at different displacement levels for each specimen. The Figure shows steady degradation. This degradation is due to the propagation and widening of the flexure cracks.

Relative to J5, the decrease in stiffness degradation rate was 5.21% for specimen J9 as shown in Figure 35. This means that stiffness degradation rate for specimen J5 is higher than J9 which means that J5 has a reduced propagation rate of crack.

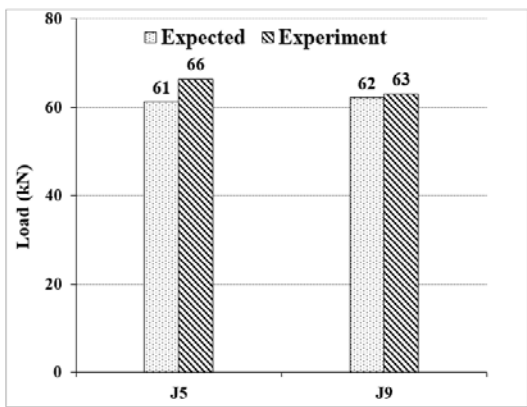
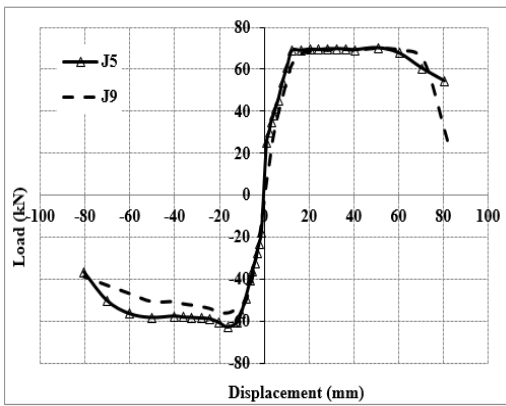


Figure 30: Load –displacement ductility envelope for group 3 Figure 31: Expected and Experimental load capacities for group 3

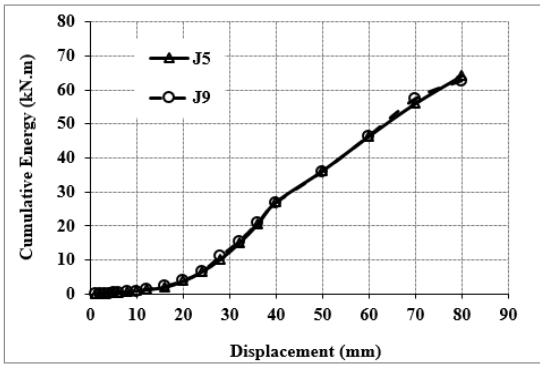
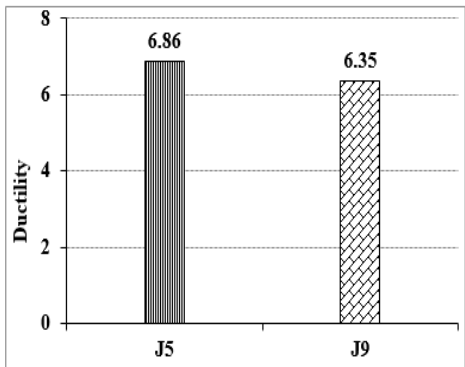


Figure 32: Displacement ductility factor for group3 Figure 33: Cumulative dissipated energy versus displacement for group 3

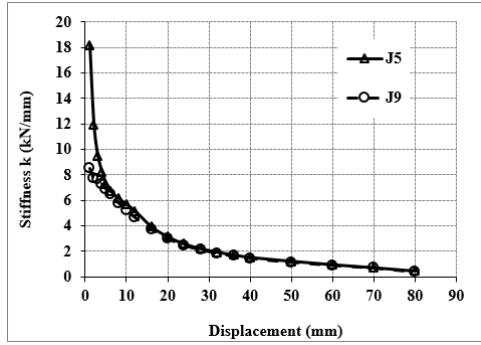


Figure 34: Stiffness degradation versus displacement for group 3

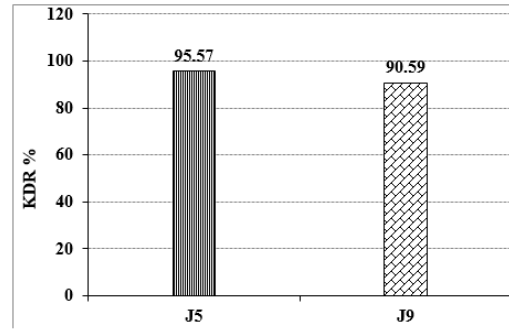


Figure 35: Stiffness degradation rate for group 3

7. CONCLUSIONS

1. Experimental program showed that the wide beam designed according to seismic precaution of the Egyptian code has well performance although beam to column width ratio was greater than two. Wide beam also performed well even when two thirds of the wide beam flexural reinforcement was anchored outside the column core. Increasing beam width with 150% and 200% lead to an increase in the lateral load capacity of 12%, and 11%, and an increase in ductility of 13%, and 32% respectively. Relative to expected capacity, the increase in lateral load capacity was 13%, 22% and 8% for specimens J1, J2 and J5.
2. Increasing reinforcement concentration inside column core decreased lateral load capacity with 4% and 5% and decreased ductility with 12% and 14 % for specimens J3 and J4. This means that specimen with uniformly distributed reinforcement has the best ability to dissipate energy and this was unlike expected result from previous research.
3. Relative to J5, decreasing number of stirrups branches decreased lateral load capacity with 5 % and decreased ductility with 7 % for specimen J9. J5 stirrups can be considered suitable reinforcement configuration for flexure member.
4. All specimens were able to sustain wide stable load displacement hysteresis loops with large area enclosed within the loops, the joint specimens showed a strong column weak beam collapse mechanism.
5. Steady Stiffness reduction for all specimens during displacement cycles due to concrete deterioration which results from the propagation and widening of the flexure cracks.
6. It is recommended that The Egyptian code change the limit of dimensions for wide beams.

8. REFERENCE

1. Egyptian Code of Practice for Design and Construction of Reinforced Concrete Structure, Housing and Building National Research Center, Giza, Egypt, ECP203, 2007.

2. ACI Committee 318, "Building Code Requirements for Structural Concrete (ACI 318-08) and Commentary," American Concrete Institute, Farmington Hills, MI, 2008, pp.473.
3. Amer M. Elsouri and Mohamed H. Harajli,. "Gravity load –designed concealed wide beam –narrow column connections: experimental assessment of seismic response" COMPDYN 2011 III ECCOMAS thematic conference on computational methods in structural dynamics and earthquake engineering Corfu, Greece, 2011.
4. Amer M. Elsouri and Mohamed H. Harajli. "Behavior of Reinforced Concrete Wide Concealed-Beam/ Narrow-Column Joints under Lateral Earthquake Loading" ACI Structural Journal, V. 110, No. 2, 2013.
5. James M. Lafave and James K. Wight, July, "Reinforced Concrete Exterior wide Beam – Column-Slab Connections Subjected to Lateral Earthquake Loading," ACI Structural Journal , Vol. 96, No. 4, 1999,pp. 577-585.
6. John S. Stehle, Helen Goldsworthy, and Priyan Mendis. "Reinforced Concrete Interior wide Band Beam – Column Connections Subjected to Lateral Earthquake Loading," ACI Structural Journal , Vol. 98, No. 3, 2001,pp. 270-278.
7. Abdel-Rahman, A. "The effective width of wide beams," Journal of the Egyptian society of engineers, Cairo, proceeding No. 4, December, 1980.
8. Bing Li and SudhhakarA. Kulkkrni. "Seismic Behavior of Reinforced Concrete Exterior wide Beam – Column Joints," Journal of Structural Engineering, Vol. 136, No. 1, 2010.
9. Amir Fateh, FarzadHejazi, AlirezaZabihiArashBehnia, " Behavior of external column- wide beam joint with different bar arrangement and existence of joint shear link under gravity" Caspain Journal of Applied Sciences Research, 2(2),January 2013,pp. 120-130.
10. Hala Metawei, "Behavior of Beam – Column Joints in Monolithic Reinforced Concrete Structure" PHD. Thesis, Faculty of Engineering, AinShams University Egypt, 1990.
11. M. Said, T.M. Elrakib, "Enhancement of Shear Strength and ductility for reinforced concrete wide beams due to web reinforcement," Journal of the Housing and Building National Research Center, February 2013.